“©2020 IEEE. Personal use of this material is permitted. Permission from IEEE must be obtained for all other uses, in any current or future media, including reprinting/republishing this material for advertising or promotional purposes, creating new collective works, for resale or redistribution to servers or lists, or reuse of any copyrighted component of this work in other works.”

Synthesizing Beam-Scannable Thinned Massive Antenna Array Utilizing Modified Iterative FFT for Millimeter-Wave Communication

Yanhui Liu, *Senior Member, IEEE*, Jinxiang Zheng, Ming Li, Qianke Luo, Yin Rui, Y. Jay Guo, *Fellow, IEEE*

***Abstract*—In this paper, a modified iterative FFT (MI-FFT) technique is presented to synthesize thinned massive array for 5G millimeter-wave communications. The periodicity of a scannable array factor for a uniformly spaced planar array is discussed and employed to reduce the complexity of array factor computation. A gradual array thinning strategy is introduced to prevent the iterative procedure from being trapped into an endless loop so that a better solution with lower sidelobe level (SLL) can be found. The beamwidth control (BWC) is also added in the MI-FFT to control the pattern beamwidth. A thinned 128-element planar array with parasitic patch covered microstrip antenna elements is designed with the frequency band from 25.2 GHz to 31.6 GHz. The 128 element positions are optimally selected from a prescribed larger layout by the proposed method, and consequently the obtained thinned array has a much lower SLL and narrower beamwidth than a conventional fully occupied 128-element array.**

***Index Terms*—Thinned massive antenna array, modified iterative FFT (MI-FFT), beam scanning, mm-wave communication.**

I. Introduction

In fifth-generation (5G) mobile networks, there is a tremendous increase in the data traffic problem due to users demands on multimedia services [1], [2]. One of the most promising techniques is using millimeter (mm)-wave communication technology since it provides high channel capacity and fast transmission rates [3]. However, the mm-wave communication suffers from high path-loss and limited scattering. To overcome these problems, massive antenna arrays have been extensively applied in mm-wave communication systems [4]–[6]. In general, use of larger array with more elements can reduce both the pattern beamwidth and the inter-beam interference so as to increase the allowable number of users for simultaneous communications. However, the increase in the number of elements will result in a high cost of the whole system.

Some techniques employing analog-digital hybrid antenna array feeding networks can reduce the cost of the whole system while maintaining the same array aperture with high radiation gain [8]–[10]. The limitation with these techniques is that they can also reduce the number of simultaneous beams due to the use of analog feeding networks on sub-array level. An alternative way of reducing the beamwidth and sidelobe level (SLL) is optimizing element positions on a relatively larger aperture. In the past, many array layout optimization methods have been presented, and they include, for example, stochastic optimization algorithms [11]–[14], sparse array reconstruction methods [15]–[19], iterative convex optimization techniques [20]–[22], and iterative fast Fourier transform (I-FFT) technique [23]–[25]. Among them, the I-FFT technique utilizing the Fourier transform relationship between the excitation distribution of an equally spaced array and its array factor would be the most efficient technique. However, the conventional I-FFT usually picks up the elements with large excitations and simply discards the elements with small excitations to accommodate a prescribed filling factor in each iteration, and consequently the iterative procedure is easily trapped into an endless loop without any improvement [23]–[25].

In this work, a modified iterative FFT (MI-FFT) is introduced to design beam-scannable thinned massive antenna arrays for mm-wave communications. In the proposed MI-FFT, the periodic property of an array factor for a uniformly spaced planar array is employed to reduce the computational complexity of a scannable beam pattern. A gradual array thinning strategy is adopted to reduce the possibility of being trapped into the endless loop so that a better solution with lower SLL can be found in the iteration process. In addition, a beamwidth control (BWC) is introduced to obtain narrower beamwidth which is useful for reducing the beam-interference in multi-user communication environment. An example of synthesizing a thinned 128-element array with parasitic-patch covered U-slot microstrip antenna elements for wide-angle beam scanning is provided to validate the effectiveness and advantages of the proposed method. Synthesis results show that the thinned 128-element array with an optimized layout has a much lower SLL and narrower beamwidth than a conventional fully occupied array with the same number of elements.

II. Formulation and Algorithm

A. Scannable array factor and its property

Consider a planar array with $M \times N$ elements uniformly arranged in a rectangular grid at distance d_x along M columns and d_y along N rows. Its array factor is given by

$$AF(u,v) = \sum_{m=0}^{M-1} \sum_{n=0}^{N-1} I_{m,n} e^{j\beta(md_x u + nd_y v)} \tag{1}$$

Manuscript received xxx. This work was supported by the Natural Science Foundation of China (NSFC) under Grant No. 61871338. (Corresponding author: Yanhui Liu)

Y. Liu, J. Zheng, Q. Luo and Y. Rui are with the Institute of Electromagnetics and Acoustics, Xiamen University, Fujian 361005, China (yanhuiliu@xmu.edu.cn).

M. Li and Y. Jay Guo are with the Global Big Data Technologies Centre, University of Technology Sydney (UTS), NSW 2007, Australia.

where

$$u = \sin\theta\cos\varphi - \sin\theta_0\cos\varphi_0 \tag{2}$$

$$v = \sin\theta\sin\varphi - \sin\theta_0\sin\varphi_0 \tag{3}$$

In the above, $I_{m,n}$ is the excitation coefficient of the (m,n)-th element, $\beta = 2\pi/\lambda$ is the wavenumber in free space where λ is the wavelength, and (θ_0, φ_0) is the beam pointing direction.

Let us consider the range of (u,v) for the scannable array factor. When the beam pointing direction is $\theta_0 = 0$ and $\varphi_0 = 0$, we have that $u = \sin\theta\cos\varphi \in [-1,1]$ and $v = \sin\theta\sin\varphi \in [-1,1]$. In this situation, the visible region of the $AF(u,v)$ can be defined as $\Omega_0 = \{(u,v); |u^2+v^2 \le 1\}$. For a more general case of beam scanning within the range of $\{(\theta_0,\varphi_0); |0 \le \theta_0 \le \theta_{\max}\ \&\ 0 \le \varphi_0 \le 2\pi\}$, the variation range of (u,v) is given by

$$\Omega_s = \{(u,v); |\sqrt{u^2+v^2} \le 1 + \sin\theta_{\max}\} \tag{4}$$

As shown in Fig. 1, the region Ω_s depending the maximum scanning angle $\theta_{\max}$ may cover some space outside of the square cell $\Omega_{\text{cell}} = \{(u,v); ||u| \le 1 \& |v| \le 1\}$.

In addition, the scannable array factor for a uniformly spaced planar array has a very interesting property that $AF(u,v)$ is a two-dimensional (2D) periodic function with periods of $T_u = 2\pi/\beta d_x$ and $T_v = 2\pi/\beta d_y$ in u- and v-dimensions, respectively. Hence, the scannable array factor can be evaluated within only one period in (u,v)-space. For example, when $d_x = d_y = \lambda/2$, we have $T_u = T_v = 2$, as shown in Fig. 1. In this situation, the scannable array factor can be calculated within the square cell Ω_{cell}, and for the part within Ω_s but outside of Ω_{cell}, we can just copy the corresponding result in Ω_{cell}. This property can be used to reduce the complexity of evaluating the scannable array factor.

B. The modified iterative FFT (MI-FFT) synthesis method

From (1), the scannable array factor defined in (u,v)-space is an inverse 2D discrete-space Fourier transform (DSFT) of the excitation distribution $\{I_{m,n}\}$. This means that the 2D inverse FFT (2D-IFFT) can be used to speed up the computation of this array factor. As is mentioned above, for a uniformly spaced planar array, the scannable array factor can be evaluated only in its one period Ω_{cell}. By setting $u = \frac{k\lambda}{Kd_x}$ $(k = -\frac{K}{2}, \cdots, \frac{K}{2}-1)$ and $v = \frac{l\lambda}{Ld_y}$ $(l = -\frac{L}{2}, \cdots, \frac{L}{2}-1)$, we obtain

$$AF(k,l) = \sum_{m=0}^{M-1}\sum_{n=0}^{N-1} I_{m,n} e^{j\frac{2\pi mk}{K}} e^{j\frac{2\pi nl}{L}} \tag{5}$$

Clearly, the above summation can be efficiently evaluated by using the 2D-IFFT. Conversely, once the array factor in one period Ω_{cell} is known, the excitation distribution $\{I_{m,n}\}$ can be efficiently obtained by performing the 2D-FFT on the array factor.

Thus, an iterative FFT (I-FFT) technique can be developed in which the forward and backward transformations between the excitation distribution and array factor are successively performed by using 2D-FFT and -IFFT and some modifications on pattern shape and/or excitation distribution are also executed in each iteration to make the synthesis result

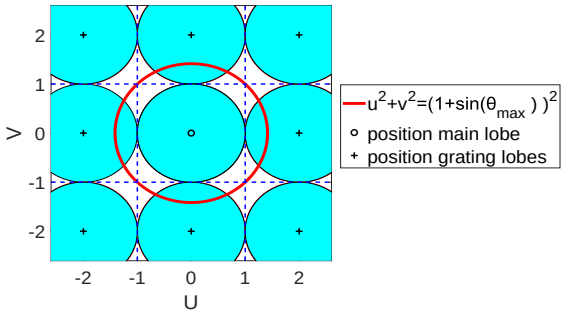

Fig. 1. The scannable array factor and its periodicity.

approaching to the desired one [26]. This idea can be further generalized to find a uniform amplitude thinned array from a predefined uniformly spaced array layout by enforcing larger excitations of selected elements to be 1 and discarding the elements with smaller excitations at each iteration [23], [24]. For example, assume that the goal is selecting Q elements from the $M\times N$-element layout. The filling factor is $f = Q/(MN)$. The I-FFT technique needs to pick up Q elements with uniform excitations in each iteration. However, in reality, the obtained excitations by performing the 2D-FFT on the $\{AF(u,v)\}$ are not exactly equal to either 1 or 0, hence the I-FFT enforces the Q larger excitations to be 1 and just discards the other $(MN-Q)$ elements with smaller excitations in each iteration. This synthesis procedure proceeds until the obtained new distribution of the selected Q elements keeps the same as that obtained at the previous iteration. Due to the crude operation by selecting only Q elements with enforced equal excitations from MN elements with continuously varied excitations, the pattern modification is sometimes not enough to cause the change of the selected element positions. This make the synthesis to be easily trapped in a local solution usually after only few iterations (e.g., less than 10 iterations). Hence, the original I-FFT presented in [23] and [24] choose to use a different initial distribution of element excitations and re-start the synthesis. In general, such a re-initialization needs to be performed several hundreds or even thousands of times to obtain a satisfactory pattern with a relatively low SLL. The other issue with the original I-FFT is lack of beamwidth control (BWC) for the synthesized pattern in the iteration and consequently the beamwidth of the obtained final pattern may be wider than what it should be for a given aperture.

To overcome the problem mentioned above, a modified iterative FFT (MI-FFT) is introduced here. A gradual array thining strategy is adopted in which much more than Q elements is chosen at the beginning and then the number of selected elements is gradually reduced as the iteration proceeds. In this situation, the distribution of the selected elements can be more easily updated by the pattern modification in each iteration, which makes the proposed procedure proceed more stably to obtain a better solution. In addition, the BWC is incorporated into the synthesis procedure by enforcing the pattern level out of the desired mainlobe region to be a prescribed SLL in the pattern modification of each iteration. The detailed procedure of the MI-FFT is provided in Algorithm 1.

Algorithm 1 The Proposed MI-FFT for Synthesizing Beam-Scannable Thinned Massive Planar Arrays

1: Set an initial mesh grid with $M \times N$ uniformly spaced potential element positions. Set the maximum beam scanning angle $\theta_{\max}$ and determine the scanning range Ω_s in the u-v space;
2: Initialize the element excitation distribution of $\{I_{m,n}\}$ ($m = 0, 1, \cdots, M-1$, $n = 0, 1, \cdots, N-1$) such that each element has a possibility of p_n to be 1 and a possibility of $(1-p_n)$ to be 0; set p_n as a positive value that is close to 1, e.g., $p_n = 0.95$;
3: Select the elements with '1' excitations, and count the number of selected elements by Q;
4: Apply $K \times L$-point IFFT on the distribution of $\{I_{m,n}\}$ to obtain the array factor $\{AF(u,v)\}$ over the rectangular region Ω_{cell} in the u-v space. By utilizing the periodicity of array factor, we can obtain all the values of $\{AF(u,v)\}$ in the scanning range Ω_s;
5: Check whether the pattern levels within Ω_s meet a desired SLL bound Γ_{SLL}, if so, adjust their magnitudes to a over-suppressed level (OSL) Γ_{OSL} and keep their phases unchanged. Γ_{OSL} is usually set to be lower than Γ_{SLL}, e.g., $\Gamma_{OSL} = \Gamma_{SLL} - 5\ dB$;
6: Check whether the pattern mainlobe is larger than the prescribed region or not. If so, adjust the pattern level out of the prescribed region to be the sidelobe level and keep the phases unchanged;
7: Apply $K \times L$-point FFT on the modified pattern $AF_{\text{mod}}(u,v)$ to obtain new excitation distribution $\tilde{I}_{m,n}$;
8: Set $Q = Q - flat[\delta Q]$ where $\delta > 0$ is a small positive value, e.g. $\delta = 0.005$, and set Q largest excitations of $\{\tilde{I}_{m,n}\}$ to 1 and others to 0;
9: Repeat Step 4 to 8 until Q reaches the required number of elements.

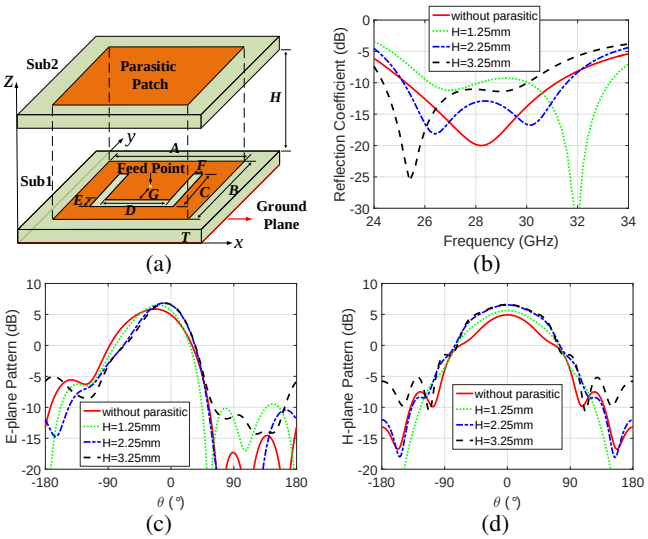

Fig. 2. The proposed parasitic-patch-covered antenna and its simulated reflection coefficient as well as radiation patterns at 28.5 GHz. (a) Geometry of the proposed antenna ($A = 3.10$ mm, $B = 2.37$ mm, $C = 1.67$ mm, $D = 1.49$ mm, $E = 0.14$ mm, $F = 0.19$ mm, $G = 0.58$ mm, $H = 2.25$ mm, $T = 1.575$ mm, $\varepsilon_r = 2.2$), (b) simulated reflection coefficient, (c) E-plane pattern and (d) H-plane pattern.

III. A Thinned Massive mm-Wave Array Design

In this section, we conduct an example of designing a thinned massive antenna array with capability of beam scanning within $\pm 20°$ in E-plane and $\pm 60°$ in H-plane which is suitable for use in conventional 5G mm-wave communications. This thinned antenna array has 128 elements whose positions are optimally selected from a predefined 24×12 mesh grid, and the element is chosen as a parasitic-patch covered U-slot microstrip antenna working in frequency band from 25.2 GHz to 31.6 GHz. The performance of this thinned antenna array and a conventional fully occupied array with the same number of elements is compared in detail.

A. Antenna element design

For an antenna working for 5G mm-wave communication, broad impedance bandwidth, high gain and high capability for beam scanning are generally required. Fig. 2(a) shows the proposed parasitic-patch-covered microstrip antenna, which consists of two substrates: the lower substrate Sub1 with a U-slot loaded patch working as the radiation antenna and the upper substrate Sub2 with a same-sized rectangular patch working as the parasitic part. The Rogers 5880 with a dielectric constant $\varepsilon = 2.2$ and a loss tangent 0.0009 is utilized for both Sub1 and Sub2. To obtain high gain and broader impedance bandwidth, we have studied the sizes of the patch and the U-slot as well as the distance between Sub1 and Sub2. Owing to the limited space, here we only provide the results about how the distance between Sub1 and Sub2 changes the impedance bandwidth and the antenna gain. The simulated reflection coefficient, E- and H-plane patterns at 28.5 GHz of the proposed antenna at different H are shown in Fig. 2(b), (c) and (d), respectively. The results for the antenna without the parasitic patch are also included in this figure. As shown in Fig. 2(b), the impedance bandwidth is increased by adding the parasitic patch. From Fig. 2(c), we can also see that after adding the parasitic patch, the beam direction of the E-plane pattern is corrected to almost the broadside direction meanwhile the maximum gain is increased from 4.92 dB to 6.53 dB. In addition, the 3 dB beamwidth in the H-plane becomes broader that is better for beam scanning in this plane. From the parameters study, we choose a proper value of $H = 2.25$ mm. With this choice, the impedance bandwidth of $S_{11} \leq 10$ dB is from 25.2 GHz to 31.6 GHz and the 3 dB beamwidth at 28.5 GHz covers the beam scanning space of $\pm 20°$ in E-plane and $\pm 60°$ in H-plane. The detailed parameters of the proposed antenna are given in Fig. 2.

B. Thinned antenna array layout design

Consider a 128-element antenna array with capability of beam scanning within $\pm 20°$ in $\varphi = 0°$-plane (E-plane) and $\pm 60°$ in $\varphi = 90°$-plane (H-plane). As shown in Fig. 3(a), a conventional choice is placing the 128 antenna elements on a $\lambda/2$-spaced 16×8 mesh grid. As shown in Fig. 4(a) and (b), its broadside pattern obtained by multiplying the broadside array factor and element pattern has the maximum SLL of -13.30 dB and the 3 dB beamwidth is $5.63°$ in $\varphi = 0°$-plane and $11.95°$ in $\varphi = 90°$-plane. When the pattern is scanned to the direction of $(\theta_0 = -60°, \varphi_0 = 0°)$, the SLL is increased to -11.89 dB and the beamwidth in $\varphi = 0°$-plane is increased to $11.25°$. When the pattern is scanned in $\varphi = 90°$-plane, the SLL and the beamwidth are also increased accordingly.

To improve the pattern performance, we optimize the antenna array layout by selecting 128 element positions from a predefined $\lambda/2$-spaced 24×12 mesh grid that provides a larger aperture with much more degrees of element position freedoms. For comparison, we apply both the original I-FFT and the proposed MI-FFT algorithms to synthesize the same example. In both of the methods, we set $\Gamma_{SLL} = -20$ dB for

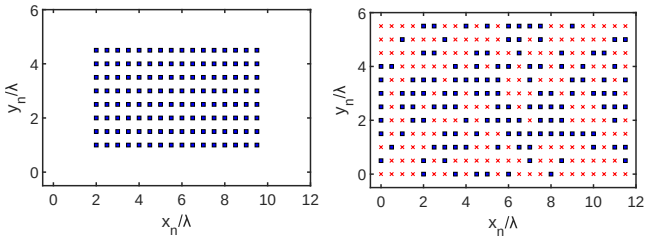

Fig. 3. Two kinds of 128-element array layouts. (a) The conventional fully-occupied array and (b) the synthesized thinned array ('□' denote a selected element).

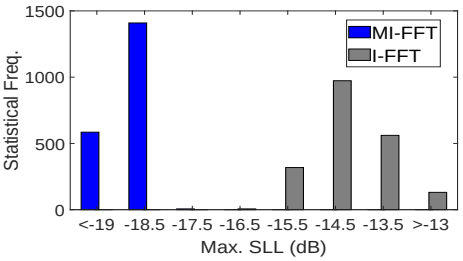

Fig. 5. The comparison of the maximum SLL histogram for 128-element thinned array.

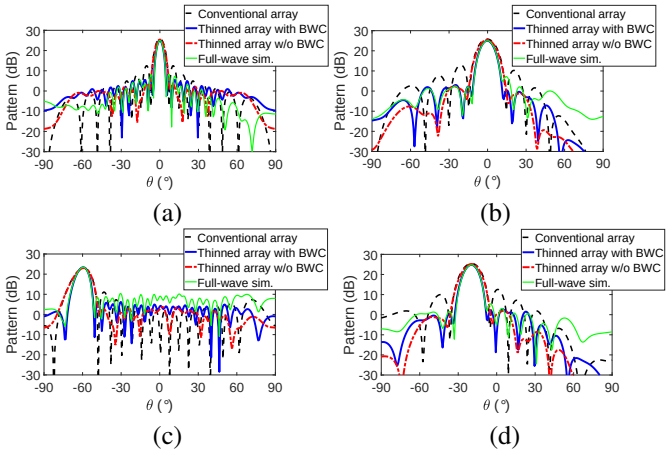

Fig. 4. The patterns of the thinned array and the conventional fully occupied array, both with 128 elements. (a) The broadside pattern in $\varphi = 0°$-plane, (b) the broadside pattern in $\varphi = 90°$-plane, (c) the scanned pattern in $\varphi = 0°$ plane with beam pointing at $(\theta_0 = -60°, \varphi_0 = 0°)$, and (d) the scanned pattern in $\varphi = 90°$ plane with beam pointing at $(\theta_0 = -20°, \varphi_0 = 90°)$. The full-wave simulated results for the thinned array obtained with BWC are also included

the desired SLL and $\Gamma_{OSL} = -25$ dB for the over-suppressed level if some pattern levels out of the desired mainlobe region are beyond the desired SLL. Since no BWC is considered in the original I-FFT, we first do not use the BWC mechanism yet in the proposed MI-FFT for fair comparison. It should be noted that in the original I-FFT, only 128 elements are selected and all other potential elements are just discarded in each iteration. In contrast, for the proposed MI-FFT, we adopt $p_n = 0.95$ and $\delta = 0.005$ for controlling the reduction in the number of selected elements. In this case, 274 elements are selected at the beginning and then the number of selected elements is gradually reduced to 128. We run each of the two methods 2000 times by using different random initial excitation distributions for comparing their statistic performances. Fig. 5 shows the histograms of the maximum SLLs of the scannable array factors for the obtained thinned 128-element arrays over 2000 runs by these two methods. It is clear that the achievable best and averaged SLLs by the proposed MI-FFT are much lower than the corresponding results by the original I-FFT. This proves the advantage of using the gradual thinning strategy other than simply discarding all other elements at the beginning.

To narrow the obtained beamwidth, we now add the BWC in the proposed MI-FFT. The obtained final array layout of the thinned 128-element array is shown in Fig. 3(b). The corresponding patterns obtained by multiplying array factors with the element pattern in broadside beam and scanned beam cases are shown in Fig. 4(a)-(d). The patterns obtained by the proposed method without BWC are also shown in this figure for comparison. As can be seen, the proposed method with/without BWC can obtain thinned arrays that have much lower SLLs than the conventional fully occupied array due to the array layout optimization over a larger aperture. Compared with the thinned array obtained without BWC, the thinned array obtained with BWC indeed significantly reduce the beamwidth while the SLL is increased not much. For the broadside beam of this thinned array, the beamwidth is $4.22°$ in $\varphi = 0°$-plane and $9.14°$ in $\varphi = 90°$-plane. They are much narrower than those of the conventional array. The relative advantages also maintain when the pattern is scanned to the direction of either $(\theta_0 = -60°, \varphi_0 = 0°)$ or $(\theta_0 = -20°, \varphi_0 = 90°)$. The full-wave simulated results for the thinned antenna array obtained with BWC are also included in Fig. 4. As can be seen, although the SLL is somehow increased especially at a large scanning angle due to the mutual coupling effect [27], the full-wave simulated results are totally in good agreement with the array factors multiplied with the element pattern. In a short, the obtained thinned array has narrower beamwidth and lower SLL than the conventional fully occupied array. Besides, the sidelobe reduction performance obtained by the proposed method is usually less sensitive to random implementation errors than the one using nonuniform excitation amplitude weighting [28].

IV. Conclusion

We have introduced a modified iterative FFT algorithm for designing a thinned antenna array with optimized layout for mm-wave communication application. The periodicity of a scannable array factor for a uniformly spaced planar array is discussed. A gradual array thinning strategy is introduced to prevent the iterative procedure from being trapped into an endless loop so that a better array layout with lower SLL can be more easily found. In addition, the beamwidth control is also applied to obtain a narrow beamwidth of the synthesized pattern. As an example, a thinned 128-element planar array working in the band from 25.2 GHz to 31.6 GHz is designed. The obtained thinned array with an optimized layout has a much lower SLL and narrower beamwidth than those of the conventional fully occupied 128-element array. This indicates that the thinned array may provide a good candidate for 5G mm-wave communication applications.

REFERENCES

[1] P. Demestichas *et al.*, "5G on the horizon: key challenges for the radio-access network," *IEEE Veh. Technol. Mag.*, vol. 8, no. 3, pp. 47–53, Sep. 2013.

[2] F. Boccardi, R. W. Heath, A. Lozano, T. L. Marzetta, and P. Popovski, "Five disruptive technology directions for 5G," *IEEE Commun. Mag.*, vol. 52, no. 2, pp. 74–80, Feb. 2014.

[3] W. Roh *et al.*, "Millimeter-Wave beamforming as an enabling technology for 5G cellular communications: theoretical feasibility and prototype results," *IEEE Commun. Mag.*, vol. 52, no. 2, pp. 106–113, Feb. 2014.

[4] F. Rusek *et al.*, "Scaling up MIMO: opportunities and challenges with very large arrays," *IEEE Signal Process. Mag.*, vol. 30, no. 1, pp. 40–60, Jan. 2013.

[5] J. Hoydis, S. Brink, and M. Debbah, "Massive MIMO in the UL/DL of cellular networks: how many antennas do we need?" *IEEE J. Sel. Areas Commun.*, vol. 31, no. 2, pp. 160–171, Feb. 2013.

[6] T. L. Marzetta, "Noncooperative cellular wireless with unlimited numbers of base station antennas," *IEEE Trans. Wireless Commun.*, vol. 9, no. 11, pp. 3590–3600, Nov. 2010.

[7] Z. Zhang and H. Yu, "Beam interference suppression in multi-cell millimeter wave communications," *Digital Commun. Networks*, pp. 1–8, Jan. 2018. [Online] Available: https://doi.org/10.1016/j.dcan.2018.01.003.

[8] A. F. Molisch *et al.*, "Hybrid beamforming for massive MIMO: A survey," *IEEE Commun. Mag.*, vol. 55, no. 9, pp. 134–141, Sep. 2017.

[9] S. Sun, T. S. Rappaport, and M. Shaft, "Hybrid beamforming for 5G millimeter-wave multi-cell networks," in *Proc. IEEE Conf. Comput. Commun. Workshops*, Apr. 2018, pp. 589–596.

[10] J. A. Zhang, X. Huang, V. Dyadyuk, and Y. J. Guo, "Massive hybrid antenna array for millimeter-wave cellular communications," *IEEE Wireless Commun.*, vol. 22, no. 1, pp. 79–87, Feb. 2015.

[11] A. Akdagli and K. Guney, "Shaped-beam pattern synthesis of equally and unequally spaced linear antenna arrays using a modified tabu search algorithm," *Microw. Opt. Technol. Lett.*, vol. 36, no. 1, pp. 16–20, Jan. 2003.

[12] D. G. Kurup, M. Himdi, and A. Rydberg, "Synthesis of uniform amplitude unequally spaced antenna arrays using the differential evolution algorithm," *IEEE Trans. Antennas Propag.*, vol. 51, no. 9, pp. 2210–2217, Sep. 2003.

[13] R. Bhattacharya, T. K. Bhattacharya, and R. Garg, "Position mutated hierarchical particle swarm optimization and its application in synthesis of unequally spaced antenna arrays," *IEEE Trans. Antennas Propag.*, vol. 60, no. 7, pp. 3174–3181, Jul. 2012.

[14] A. Darvish and A. Ebrahimzadeh, "Improved fruit-fly optimization algorithm and its applications in antenna arrays synthesis," *IEEE Trans. Antennas Propag.*, vol. 66, no. 4, pp. 1756–1766, Apr. 2018.

[15] Y. Liu, Z. Nie, and Q. H. Liu, "Reducing the number of elements in a linear antenna array by the matrix pencil method," *IEEE Trans. Antennas Propag.*, vol. 56, no. 9, pp. 2955–2962, Sep. 2008.

[16] Y. Liu, Q. H. Liu, and Z. Nie, "Reducing the number of elements in the synthesis of shaped-beam patterns by the forward-backward matrix pencil method," *IEEE Trans. Antennas Propag.*, vol. 58, no. 2, pp. 604–608, Feb. 2010.

[17] Y. Liu, Q. H. Liu, and Z. Nie, "Reducing the number of elements in multiple-pattern linear arrays by the extended matrix pencil methods,"*IEEE Trans. Antennas Propag.*, vol. 62, no. 2, pp. 652–660, Feb. 2014.

[18] H. Shen and B. Wang, "Two-dimensional unitary matrix pencil method for synthesizing sparse planar arrays,"*Digit. Signal Process.*, vol. 73, pp. 40–46, 2018.

[19] F. Viani, G. Oliveri, and A. Massa, "Compressive sensing pattern matching techniques for synthesizing planar sparse arrays," *IEEE Trans. Antennas Propag.*, vol. 61, no. 9, pp. 4577–4587, Sep. 2013.

[20] G. Prisco and M. D'Urso, "Maximally sparse arrays via sequential convex optimizations," *IEEE Antennas Wireless Propag. Lett.*, vol. 11, pp. 192–195, 2012.

[21] B. Fuchs, "Synthesis of sparse arrays with focused or shaped beampattern via sequential convex optimizations," *IEEE Trans. Antennas Propag.*, vol. 60, no. 7, pp. 3499–3503, Jul. 2012.

[22] P. You, Y. Liu, S. L. Chen, K. D. Xu, and Q. H. Liu, "Synthesis of unequally spaced linear antenna arrays with minimum element spacing constraint by alternating convex optimization," *IEEE Antennas Wireless Propag. Lett.*, vol. 16, pp. 3126–3130, 2017.

[23] W. P. M. N. Keizer, "Linear array thinning using iterative FFT techniques," *IEEE Trans. Antennas Propag.*, vol. 56, no. 8, pp. 2757–2760, Aug. 2008.

[24] W. P. M. N. Keizer, "Large planar array thinning using iterative FFT techniques," *IEEE Trans. Antennas Propag.*, vol. 57, no. 10, pp. 3359–3362, Oct. 2009.

[25] Y. Liu, Q. Luo, M. Li, and Y. Jay Guo, "Thinned massive antenna array for 5G millimeter-wave communications," *13th Eur. Conf. on Antennas and Propagation (EuCAP)*, Krakow, Poland, Apr. 2019, pp. 1–4.

[26] W. P. M. N. Keizer, "Fast low-sidelobe synthesis for large planar array antennas utilizing successive fast fourier transforms of the array factor," *IEEE Trans. Antennas Propag.*, vol. 55, no. 3, pp. 715–722, Mar. 2007.

[27] X. Chen, S. Zhang, and Q. Li, "A review of mutual coupling in MIMO systems," *IEEE Access*, vol. 6, pp. 24706–24719, 2018.

[28] A. Zaghloul, "Statistical analysis of EIRP degradation in antenna arrays," *IEEE Trans. Antennas Propag.*, vol. 33, no. 2, pp. 217–221, Feb. 1985.